CrossMark

ORIGINAL PAPER

Waxberry-like magnetic porous carbon composites prepared from a nickel-organic framework for solid-phase extraction of fluoroquinolones

Qiong Wang[1] · Yang Wang[1] · Zhenzhen Zhang[1] · Yao Tong[1] · Lei Zhang[1]

Abstract A unique waxberry-like magnetic hierarchical porous carbon hybrid was synthesized from a nickel based metal–organic framework (Ni-MOF) which, on calcination, produces hierarchical Ni/NiO nanocrystals covered with graphitic carbon (GrC). The material was applied to magnetic solid phase extraction (MSPE) of trace levels of four fluoroquinolones (FQs) from environmental water samples. It is shown to exhibit superior extraction capability for four FQs, because the novel 3D morphology provides an enhanced surface area along with transport channels, while Ni and graphitic carbon as potential adsorption sites are ideal components. The material with inherent magnetism is reusable and displays superb recycling stability for the adsorption and desorption (by using alkaline methanol) of FQs after 6 cycles. The FQs were quantified by HPLC with UV detection, and the limits of detection (at an S/N ratio of 3) range between 7.9 and 57 ng·L^{-1}. Recoveries from spiked environmental water samples are between 88.8 and 103.7%.

Electronic supplementary material The online version of this article (doi:10.1007/s00604-017-2438-2) contains supplementary material, which is available to authorized users.

✉ Lei Zhang
zhanglei63@126.com

1 College of Chemistry, Liaoning University, 66 Chongshan Middle Road, Shenyang, Liaoning 110036, People's Republic of China

Introduction

Fluoroquinolones (FQs), as a kind of antibiotics, have been extensively used in clinical applications for human and veterinary diseases [1–4]. They can prevent the synthesis of bacterial DNA, because of the presence of F atom and piperazinyl group [5]. Compared with other antibiotics, FQs have lower solubility, bioavailability, biodegradation rates, and more likely to accumulate in sediment [6], they cannot be efficiently removed from environment water using traditional wastewater treatment processes. Unfortunately, they have been found in various real water samples, such as hospital sewage, treated sewage, and surface water bodies [7, 8]. FQs residues are making their way into food chains and reaching the consumers [9]. Therefore, monitoring FQs at trace levels in a simple and sensitive method is significant.

The environmental monitoring of FQs is a vital task, with regard to water system, usually the low level determination necessitate a pre-concentration process before analysis. Magnetic solid-phase extraction (MSPE), which has captured much attention for trace determination of multifarious analytes in consideration of its reduced consumption of organic solvents, low cost and high enrichment factors [10]. Magnetic enrichment material can be dispersed into the matrix directly and separated from samples by an external magnetic field without extra filtration or centrifugation, which makes the sample pretreatment faster and easier.

Magnetic carbon material, as an extraordinarily wonderful adsorbent with superb adsorption and recyclable properties, has been studied and applied extensively, such as $Fe_3O_4NPs@GO$ [11], C_3N_4/Fe_3O_4 [12], mag-MWCNTs [13, 14], $Fe_3O_4@PVBC@IDA-Ni$ [15] and $Fe_3O_4@SiO_2@C/N$ [16] were synthesized and used for pre-concentration environmental pollutants. Metal–organic frameworks (MOFs), as newly emerging porous materials with

large surface area, low density and ultrahigh porosity, have attracted researchers attention and adopted for widespread applications in many fields, including sensing, luminescence, drug delivery, gas storage/separation and catalysis [17, 18]. In addition, Many efforts have led to the development of MOFs as templates/precursors to construct metal and/or metal oxide nanoparticles embedded in the carbon matrix, such as Fe_3O_4@MIL-101 [19], Fe@MOF-5 [20] and Fe_3O_4@MIL-100 [21] were applied to solid-phase extraction of organic contaminants. However, the above MOF-derived porous carbons are non-magnetic, and the magnetic properties (Fe_3O_4/Fe) were reinvested by extra synthetic process, which was complex and least environmentally friendly. In this regard, a kind of MOF derived nanoporous carbons with inherent magnetism were synthesized, such as Zn-Co-ZIF nanoparticles for magnetic solid phase extraction of flunitrazepam [22]. As far as we know, Ni-MOF derived waxberry-like magnetic hierarchical porous carbon hybrid with high specific surface area used as adsorbent for solid-phase extraction was not reported.

In this paper, a magnetic hierarchical porous carbon hybrid was synthetized from a nickel-based metal-organic framework (Ni-MOF) through pyrolysis process. The resulting hierarchical Ni/NiO nanocrystals are covered with a graphitic carbon (GrC) nanocomposite. Moreover, WMHP-Ni/NiO@GrC with excellent inherent magnetism, can be collected from the matrix by an external magnetic field, economically feasible and more efficient. Remarkably, WMHP-Ni/NiO@GrC nanocomposite as effective adsorbents exhibited satisfactory extraction performance in the simultaneous determination of four FQs by high performance liquid chromatography (HPLC). Furthermore, the MSPE method was successfully used for extraction of FQs residues in environmental water samples.

Experimental

Reagents and chemicals

Fluoroquinolones (FQs), including enrofloxacin (ENR, 98% purity), norfloxacin (NOR, 98% purity), lomefloxacin (LOM, 98% purity), and ciprofloxacin hydrochloride (CIP, 98% purity) were from Tianjin HEOWNS Biochem LLC (China, www.heowns.com), and their chemical structures were shown in Fig. S1. Humic acid (90% purity) were from Shanghai Aladdin Biotechnology Co., (China, www.aladdin-e.com). Trimesic acid (H_3BTC, 98% purity), Nickel nitrate hexahydrate (Ni(NO_3)$_2$ •$6H_2O$, 98% purity), polyvinylpyrrolidone K-30 (PVP), HPLC grade acetonitrile (ACN), N,N-dimethylformamide (DMF) and Other chemicals were analytical reagent and from Sinopharm Company (China, www.sinoreagent.com).

Instruments

Micro-structure of materials was investigated in a field emission scanning electron microscope (SEM, HITACHI SU8000, Japan). The crystalline phases in the composite were confirmed by X-ray diffraction (XRD, Siemens D5000, Germany). The BET surface area was estimated by N_2 adsorption/desorption isotherm in a Micromeritics Tristar 3020 (Norcross, GA). Electronic state of ions of WMHP-Ni/NiO@GrC were analysed by X-ray photoelectron spectroscopy (XPS, Thermo ESCALAB 250Xi, USA). Raman spectras of composite were measured by Laser Confocal Micro-Raman Spectroscope (LabRAM XploRA, HORIBAJOBINYVONS.A.S, France). The FT-IR spectra were acquired on a Nicolet 330 FT-IR (Nicolet, USA). The zeta potential of adsorbent was taken with a zetasizer Nano-ZS90 apparatus (Malvern.UK). Vibrating sample magnetometer (VSM, Lakeshore 7407, USA) was used to measure the magnetic prosperities of WMHP-Ni/NiO@GrC in the field of ±20 KOe at room temperature. Quantitative analysis were completed using high performance liquid chromatography (HPLC, Simadzu Instruments Manufacturing, Co., Ltd., Japan). The pH values of solutions were measured by PHSJ-4F Model pH meter (Shanghai instrument electric science instrument, China).

Preparation of Ni-MOF precursor and WMHP-Ni/NiO@GrC

The Ni-MOF precursor was synthesized by hydrothermal method [23]. Firstly, 0.864 g Ni(NO_3)$_2$·$6H_2O$, 0.3 g H_3BTC, and 3 g PVP were dissolved in 60 mL of mixture solution (double-distilled water: ethanol: DMF = 1:1:1 v/v/v) and stirring constantly for 30 min. Secondly, the homogeneous suspension was poured into a 100 mL Teflon-lined autoclave and reaction for 10 h at 150 °C. At last the pale green products were washed with ethanol and dried in an oven for 12 h at 60 °C.

The pale green Ni-MOF precursor powders were heated to 450 °C with a ramp-rate of 1 °C·min^{-1} and maintained 30 min. The whole annealing process was carried out in a tube furnace at N_2 atmosphere. The resulting black powders were WMHP-Ni/NiO@GrC nanocomposite. The synthesis processes was illustrated in Scheme 1.

Sample preparation

For evaluate the applicability of the method, two kinds of environment water samples were analyzed. River water sample was collected from Xinkai River (Shengyang) and Seawater sample was collected from Bayuquan Bay, these
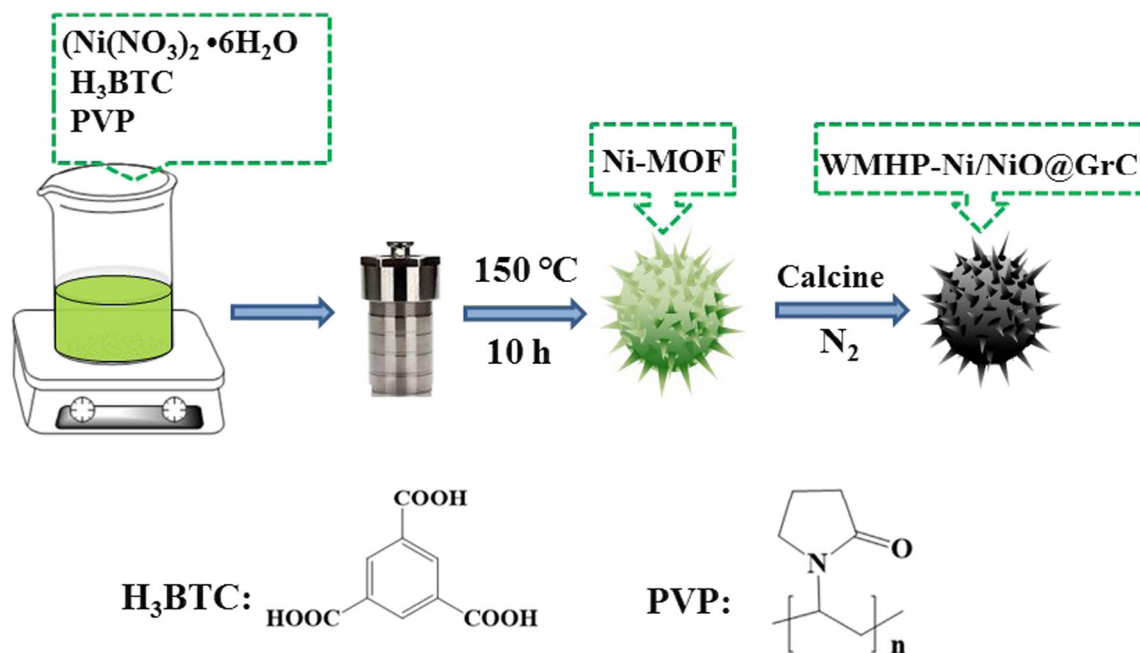
Scheme 1 The synthesis processes of WMHP-Ni/NiO@GrC

samples were stored below 4 °C after filtered through 0.45 μm nylon for later use.

MSPE procedures

The MSPE procedure was carried out as follows: 25 mL working standard solution with 25 mg WMHP-Ni/NiO@GrC were placed on a shaker at a stirring rate of 200 rpm and allowed to equilibrate for 10 min. After extraction, the WMHP-Ni/NiO@GrC was isolated from the solution using an external magnet. The target compounds were ultrasonically eluted with 1.0 mL of methanol/NaOH (1 mol· L^{-1}) (4/6, v/v) for 10 min. Eluent was separated from the WMHP-Ni/NiO@GrC by a magnet and filtered through a 0.45 μm PTFE filter membrane for HPLC analysis. Each stock solution of four FQs were obtained by dissolving 0.5 g of drug into 0.1 mol·L^{-1} HCl (0.5 mL), then diluting to 500 mL with double-distilled water and refrigerated at 5 °C, 2 ppm of four FQs mixed solution were prepared as working standard solution. The extraction process was shown in Scheme 2.

Chromatography

The HPLC analyses were performed by a Shimadzu LC-16 HPLC system equipped with SPD-16 UV detector. Chromatographic separation of four FQs was performed on an ODS-SP-C18 (150 mm × 4.6 mm, 5 μm) column (Simadzu, Japan) and the injection volume was 20 μL. The mobile phase was a mixture of triethylamine phosphate (1.5‰, pH 3 ± 0.1)–acetonitrile (83/17, v/v) delivered at a flow rate of 1.0 mL·min^{-1}, and the detection wavelength was 276 nm, column temperature was 30 °C.

Results and discussion

Characterization of adsorbent

SEM analysis was carried out to observe the morphological characteristics of the Ni-MOF precursor and WMHP-Ni/NiO@GrC. As shown in Fig. 1a, the Ni-MOF precursor exhibits obvious 3D waxberry-like structure with a submicrometer size of 3 μm, magnification of the Ni-MOF precursor was shown in Fig. 1b, the spinals grown on the surface of the sphere with an average diameter of less than 100 nm. After calcination treatment, the organic linker in the MOF scaffold would be decomposition and carbonization to produce the corresponding carbons, along with hierarchical NiO/Ni nanocrystals produced and covered with the carbons shell, and the final WMHP-Ni/NiO@GrC composites maintained the original micro-spherical hierarchical structure of the Ni-MOFs precursor (Fig. 1c). In addition, as shown in Fig. 1d, the magnetic properties of WMHP-Ni/NiO@GrC analyzed by room temperature VSM with −20.0 kOe≤H≤20.0 kOe field. The value of saturation magnetization (Ms) is about 33.71 emu·g^{-1} (inset: the photo of magnetic separation), which was enough for magnetic separation.

The phase purity of Ni-MOF precursor and WMHP-Ni/NiO@GrC were studied using X-ray diffraction (XRD) patterns. As shown in Fig. 2a, the Ni-MOF precursor is still

Scheme 2 The diagram of procedure for MSPE of four FQs
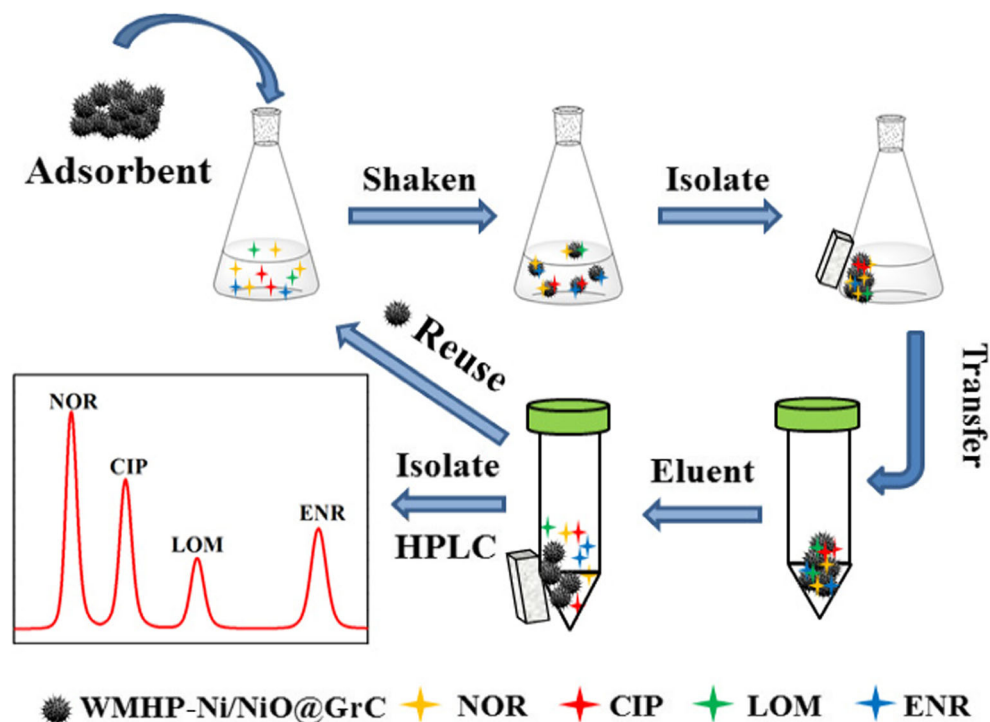
retains the original structure. After calcination, the organic linker undergo decomposition and carbonization, the metal ions (Ni^{2+}) transform to NiO_x or Ni. WMHP-Ni/NiO@GrC display obvious XRD diffraction patterns, the peaks at the 2θ values of 44.88° and 52.16° are correspond to (111) and (200) crystal planes of cubic Ni (JCPDS 4–0850), and the peaks at 44.53° and 76.63° are correspond to (200) and (220) crystal planes of NiO (JCPDS No. 78–0429), which are in agreement with other references of Ni-MOF [23]. Furthermore, an additional broad peak appeared in WMHP-Ni/NiO@GrC at nearly 25°, which can explain the presence of graphitic carbon [24]. No other phases appeared at XRD diffraction pattern, demonstrates the high purity of the sample.

XPS was used to further investigate the chemical compositions and the bonding states of the WMHP-Ni/NiO@GrC. The results prove the presence of C, O, and Ni elements. As shown in C 1 s spectra (Fig.S2A), a dominant peak at 284.6 eV ascribe to C-C bonds and relate to the sp^2 hybridized

Fig. 1 The SEM images of Ni-MOF precursor (**a**) (insert: the picture of Waxberry); the part enlargement of Ni-MOF precursor (**b**); WMHP-Ni/NiO@GrC (**c**); VSM image of WMHP-Ni/NiO@GrC (**d**) (insert: the picture of magnetic property)
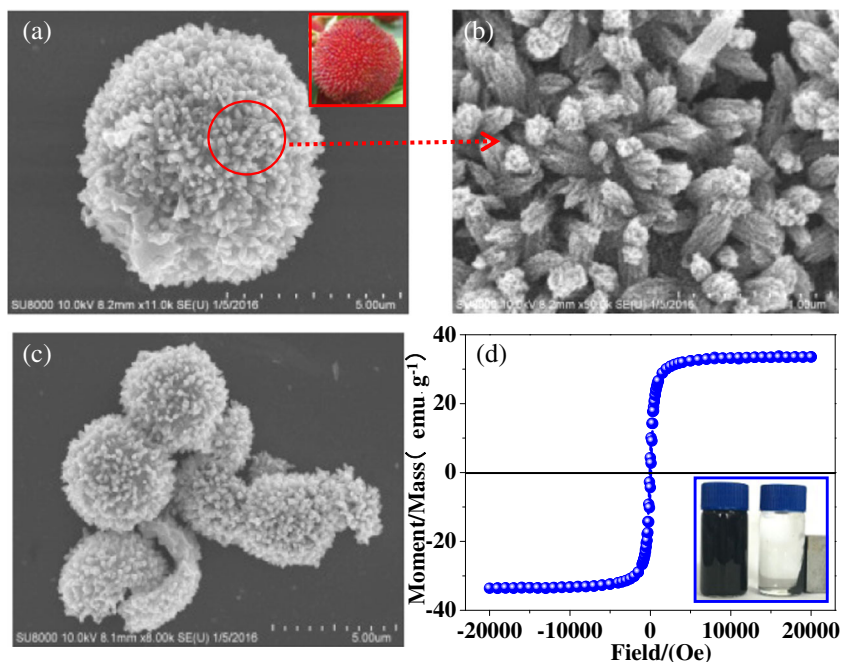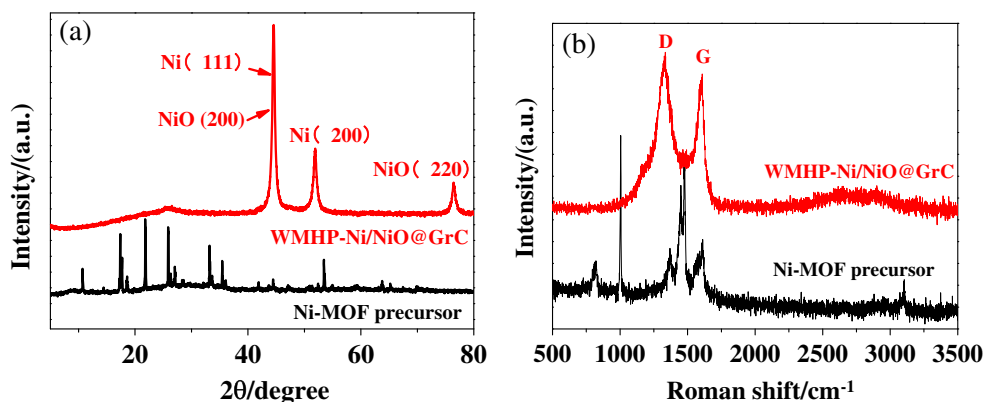
Fig. 2 (**a**) The XRD patterns of Ni-MOF precursor and WMHP-Ni/NiO@GrC; (**b**) Raman spectrum of Ni-MOF precursor and WMHP-Ni/NiO@GrC

graphite-like carbon atom in graphene [17], several weak peaks are assigned to C-O (286.9 eV), and C = O (288.5 eV). The O 1 s spectra (Fig.S2B) show that the peak at 533.8 eV is assigned to C-O bond, the binding energy peak at 532.4 eV and 530.1 eV are contributed to the presence of C=O bond, and metal–oxygen (Ni-O) bond, also suggests that the presence of lattice oxygen and oxygen-containing groups in WMHP-Ni/NiO@GrC. Likewise, the Ni 2p spectra [25] (Fig.S2C), reveal two major peaks centred at around 870.1 and 852.8 eV with a spin-energy separation of 17.3 eV, contribute to the presence of Ni $2p_{1/2}$ and Ni $2p_{3/2}$, which are characteristic peaks of Ni^{2+}, other two peaks centred at around 874.3 and 856.8 eV corresponded to Ni NPs, which are in good agreement with previous XRD result.

The graphitic structures of Ni-MOF precursor and WMHP-Ni/NiO@GrC were further examined by Raman spectroscopy. As shown in Fig. 2b, the Ni-MOF precursor is not display obvious, intense characteristic Raman band. In turn, WMHP-Ni/NiO@GrC show two characteristic Raman bands belong to graphitic carbon: D band and G band. The result is consistent with XRD diffraction patterns [26].

According to the nitrogen adsorption − desorption isotherm measurements (Fig.S3), the surface area of WMHP-Ni/NiO@GrC is 110 $cm^2 \cdot g^{-1}$, and pore-size is mainly distributed around 12 nm. The large surface area, and abundant porosity,

enhances the contact area and channel between adsorbent and the analytes, which are favorable for the extraction.

Optimization of method

For achieving the satisfied extraction efficiency, the following parameters were optimized: (a) Sample pH value; (b) Absorbent amount; (c) ionic strength (d) shake time. Respective data and Figures are given in the Electronic Supporting Material. We found the following experimental conditions to give best results: (a) A sample pH value of pH 6.0 (Fig.S4A); (b) WMHP-Ni/NiO@GrC amount of 25 mg (Fig.S4B); (c) no NaCl was added (Fig.S4C); (d) shake time of 10 min (Fig.S4D).

Interaction mechanism for the adsorption of FQs on WMHP-Ni/NiO@GrC

FQs are ampholyte compounds, the pKa values of the four FQs ranging from 8.30 to 8.89 was for the piperazinyl group and from 5.90 to 6.23 was for the carboxylic functions [27], the existing forms of FQs were influenced by the pH value of solution. When solution pH was below 6.0, FQs existed as a cation, at pH between 6.2 and 8.8, existed primarily in intermediate forms no net electrical charge and anion from solution

Fig. 3 (**a**) Zeta potential of WMHP-Ni/NiO@GrC at different pHs; **b** FT-IR spectra of WMHP-Ni/NiO@GrC (*a*), FQs (*b*), FQs-adsorbed WMHP-Ni/NiO@GrC (*c*)
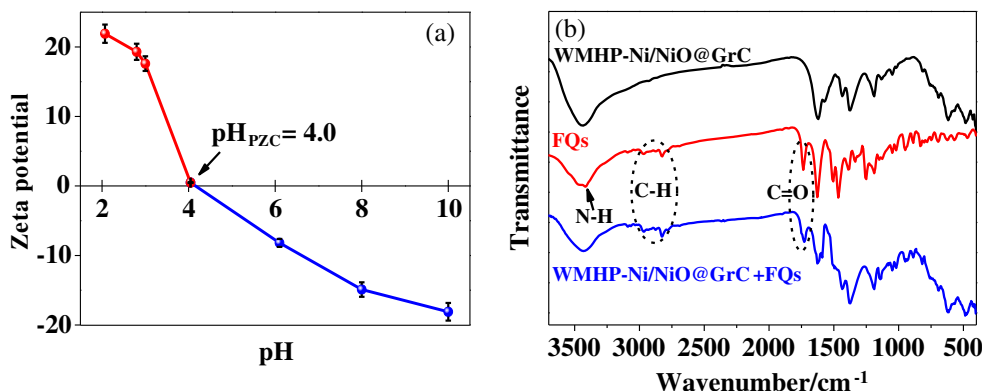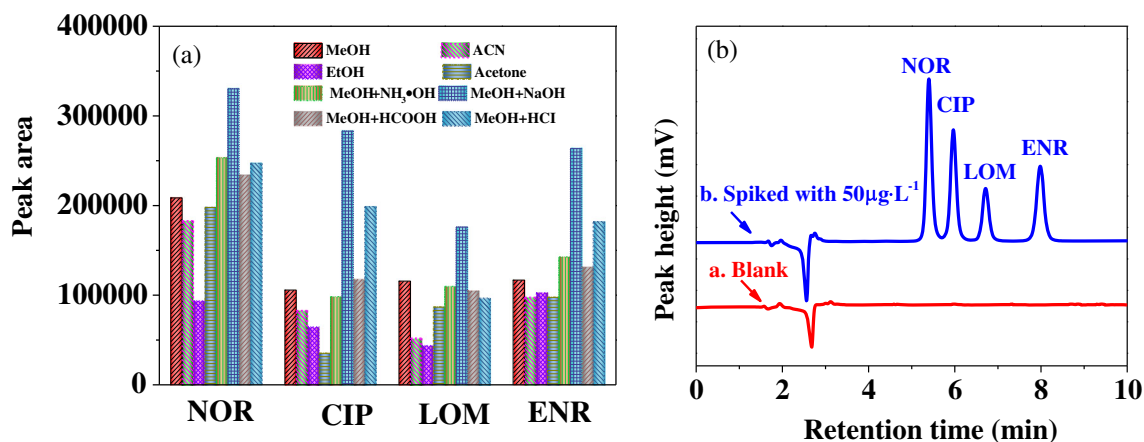
Fig. 4 **a** Effect of the desorption solvent on the recoveries of four FQs (absorbent amount: 25 mg; FQs solution concentrations: 2 mg·L^{-1}; solution volume: 25 mL; extraction time: 10 min). (**b**) HPLC-UV Chromatograms obtained at 276 nm. (*a*) Blank river water sample after pretreatment by MSPE; (*b*) The spiked river water sample (50.0 µg·L^{-1}) after pretreatment by MSPE. (WMHP-Ni/NiO@GrC: 25 mg; FQs concentrations: 2 mg·L^{-1}; sample volume: 25 mL)

pH greater than 8.8. Combining the study of zeta potential, as shown in Fig. 3a, the isoelectric point of WMHP-Ni/NiO@GrC is 4.0. WMHP-Ni/NiO@GrC present negative charges while pH > pH$_{pzc}$, FQs exist in cationic forms while the pH value from 2.0 to 6.0 [28]. Therefore, it would result in electrostatic interactions between cationic forms FQs with negative charge on the surface of WMHP-Ni/NiO@GrC. In order to further investigate the interaction mechanism between FQs and WMHP-Ni/NiO@GrC, FT-IR spectra was studied. As shown in Fig. 3b, the new peak on curve c at 1715 cm^{-1} is assigned to carbonyl group of ketone and peaks from 2800 to 2975 cm^{-1} are assigned to C-H band stretching vibration of alkane, indicating that WMHP-Ni/NiO@GrC effectively adsorbed FQs. The characteristic peak of -OH is broadened and weaken, and exhibited shifts from 3442 to 3426 cm^{-1}, suggested that FQs was attached to WMHP-Ni/NiO@GrC through H-bonding. The bands assigned to vibrational stretching frequencies of C = C at 1637 and 1618 cm^{-1} are shifted to 1627 and 1605 cm^{-1} [29], which demonstrated the π-π conjugate effect between FQs and WMHP-Ni/NiO@GrC are presented in the adsorption process and influenced the electronic cloud distribution of the molecule. In addition, FQs contained hydroxyl functional groups and amide groups, WMHP-Ni/NiO@GrC contained abundant Ni (II) sites, the

characteristic peak of N-H at 3417 cm^{-1} on curve c disappeared confirmed that the interactions between FQs and WMHP-Ni/NiO@GrC become possible through the coordinated covalent bonds [30]. Therefore, it can be deduced the interaction mechanism between FQs and WMHP-Ni/NiO@GrC was hydrogen bond, complexation, π–π interaction and electrostatic interaction.

Desorption conditions

The type of eluent directly affects the recovery of analytes. In order to obtain higher recovery, several eluents (methanol, acetonitrile, ethanol, acetone, methanol/5% NH$_3$·OH, methanol/NaOH (1 mol·L^{-1}) (6/4, v/v), methanol/HCOOH (9/1, v/v), methanol/HCl (1 mol·L^{-1}) (5/5, v/v)) were investigateds. As shown in Fig. 4A, methanol/NaOH (1 mol·L^{-1}) (6/4, v/v) exhibited the best desorption efficiency, which were in accordance with the pH result. Hence, methanol/NaOH (1 mol·L^{-1}) (6/4, v/v) was chosen as the eluent.

In order to totally desorbing the FQs from the adsorbent and achieve satisfactory recoveries, the influence of desorption time and eluent volume on desorption efficiency were investigated. The volume of eluent was investigated ranging from 0.5 to 5.0 mL. Results showed most of

Table 1 Analytical performance for FQs obtained by MSPE-HPLC-UV

Analytes	Linear range (µg·L^{-1})	r	LOD (µg·L^{-1})	LOQ (µg·L^{-1})	RSD(%)(n = 6)	
					Intra-day	Inter-day
NOR	0.10–500.00	0.9928	0.043	0.143	4.71	8.30
CIP	0.10–500.00	0.9986	0.007	0.026	7.92	6.27
LOM	0.10–500.00	0.9983	0.057	0.189	5.11	3.63
ENR	0.10–500.00	0.9977	0.028	0.933	5.32	9.47

Table 2 Analytical results for the real samples

Analytes	Spileked($\mu g \cdot L^{-1}$)	River water			Sea water		
		Found [a] ($\mu g \cdot L^{-1}$)	R%	RSD%	Found [a] ($\mu g \cdot L^{-1}$)	R%	RSD%
NOR	0	nd	–	–	nd	–	–
	50	47.78	95.6	2.71	45.53	91.1	4.31
	300	311.02	103.7	3.16	307.22	102.4	2.16
CIP	0	nd	–	–	nd	–	–
	50	50.82	101.6	4.62	48.74	97.5	5.63
	300	298.60	99.5	3.51	297.05	99.0	3.75
LOM	0	nd	–	–	nd	–	–
	50	46.36	92.7	2.84	53.16	106.3	4.16
	300	286.25	95.4	3.39	277.62	92.5	3.50
ENR	0	nd	–	–	nd	–	–
	50	44.83	89.7	4.10	51.07	102.1	3.92
	300	289.97	96.7	2.95	266.31	88.8	2.81

nd not detected

[a] Mean of three measurement

the FQs can be desorbed from the sorbent with 1 mL of eluent. The influence of desorption time was investigated, and the recoveries of the FQs evidently increased with increasing desorption time from 5 to 10 min, while maintained with time elapsing. Thus, 1 mL methanol/NaOH (1 $mol \cdot L^{-1}$) (6/4, v/v) eluent and 10 min of desorption time were chosen for the further experiments.

Interference and regeneration studies

In order to evaluate the influence of co-existing ions and organic matter, Cl^-, HCO_3^-, PO_4^{3-}, NO^{3-}, Mg^{2+}, Cu^{2+}, Cu^{2+}, Zn^{2+}, Ni^{2+}, Pb^{2+}, Na^+, K^+, and humic acid were selected as possible interfering ions. The results indicated that no obvious changes in recoveries of four FQs were found after added the interfering ions (0–10 $mg \cdot L^{-1}$) and humic acid (3 $mg \cdot L^{-1}$) into the samples, proving that the potential application of WMHP-Ni/NiO@GrC as adsorbents for magnetic solid-phase extraction of four FQs in environment water samples.

To test the regeneration of WMHP-Ni/NiO@GrC, six times adsorption/desorption cycles were carried out. The result illustrated the WMHP-Ni/NiO@GrC can be used for six cycles with lost less than 9.8% of its recovery on average, indicated that this magnetic adsorbent was stable and durable during the MSPE procedure.

Method validation

Enrichment factor (EF) is an important indicator to measure the sensitivity of method, and it can be calculated by the following equations:

$$EF = c_a/c_s \qquad (1)$$

where c_a and c_s are the concentrations of the target compounds in eluent and sample solutions, respectively.

The effect of sample volume on quantitative analysis of the four FQs was investigated in the range from 25 to 250 mL with the constant amount of each target analytes (20 μg).

Table 3 Comparison of the proposed method with other method for the determination of FQs

Method	Samples	Linear range ($\mu g \cdot L^{-1}$)	LOD ($\mu g \cdot L^{-1}$)	Recovery%	EF	Ref.
Silica-supported carbon material combined with HPLC-UV detection	water	0.1–1	0.001	70–116	125	[31]
Supported liquid membrane extraction with single hollow fiber	water	0.01–4	0.01–0.02	70–80	100	[8]
IL-FM for solid-phase extraction by HPLC	urine	50–20,000	3.5–7.3	93.6–103.7	–	[32]
Colorimetric aptamer based assay	milk	0–165.5	0.39	93.7–106.8	–	[33]
MSPE-HPLC	river/sea water	0.10–500.00	0.007–0.057	88.8–103.7	200	This work

Then, the MSPE procedure was performed under the optimum conditions, and the extraction efficiencies of four FQs ranged from 86.1 to 95.5% with the sample volumes up to 200 mL. When the sample volume was above 200 mL, the extraction efficiency was reduced to less than 80%. Combining on the result of eluent volume experimentation, it was found that the EF is about 200 under optimal conditions, shown excellent pre-concentration ability.

The linearity and intra-day and inter-day precision of the method were evaluated under the optimal conditions. The calibration curves were obtained by plotting the peak area of FQs spiked in aqueous solutions versus the concentrations (NOR: $y = 7,303,760x + 30,365$ ($r = 0.9928$); CIP: $y = 9,175,330x + 32,429$ ($r = 0.9986$); LOM: $y = 5,189,720x + 8489$ ($r = 0.9983$); ENR: $y = 8,139,230x + 51,669$ ($r = 0.9977$)), and other results were summarized in Table 1. Satisfying linearity was got in the range of 0.10–500.00 μg·L^{-1} for four FQs, and the RSDs were more than 0.9928. The limit of detection (LOD) (S/N = 3) and limit of quantification (LOQ) (S/N = 10), were in the range of 7.9–57 ng·L^{-1} and 26–189 ng·L^{-1}, respectively.

The intra-day and inter-day precisions of the MSPE method were evaluated by measuring different concentrations of FQs at 50, 100, and 300 μg·L^{-1}. Six-parallel experiments in a day obtained the intra-day RSDs, while the inter-day RSDs were obtained by the detection during three consecutive days. The results indicated that the intra-day and inter-day RSDs were below 7.92 and 9.47%, indicating the satisfying repeatability was obtained.

Sample analysis

The method was further used for the analysis of FQs in real samples (river water and sea water). As listed in Table 2, the average recoveries were 88.8–103.7% with the RSD less than 5.63. Figure 4B shows the chromatograms of samples without or with spiked standard solution, no significant interference peaks are found at the retention time of FQs.

Comparison with other reported method

The comparative study result of this work to other works was listed in Table 3. It indicated that the present method showed high sensitivity, wide linearity range and satisfactory recoveries. In addition, this work showed small solvent consumption, eco-friendly, and low cost. Thus, the MSPE method is better for the extraction and determination of FQs in real samples.

Conclusion

In this study, novel Waxberry-like magnetic hierarchical porous carbon hybrid (WMHP-Ni/NiO@GrC) was synthesized

and used as MSPE adsorbent for the simultaneous determination of four FQs by HPLC with UV detection. The MSPE method achieved effective extraction efficiency, short extraction times, high enrichment effects, and low detection limits. It has been successfully applied for the analysis of trace FQs in environmental water samples, demonstrates a fantastic application potential for the determination of FQs, and the feasibility of using this procedure for determination FQs in other complex sample is still underway.

References

1. Marouzi S, Sharifi Rad A, Beigoli S, Teimoori Baghaee P, Assaran Darban R, Chamani J (2017) Study on effect of lomefloxacin on human holo-transferrin in the presence of essential and nonessential amino acids: Spectroscopic and molecular modeling approaches. Int J Biol Macromol 97:688–699. doi:10.1016/j.ijbiomac.2017.01.047

2. Kamble R, Sharma S, Mehta P (2017) Norfloxacin mixed solvency based solid dispersions: In-vitro and In-vivo investigation. J Taibah Univ Sci. doi:10.1016/j.jtusci.2016.11.003

3. Jiang WT, Chang PH, Wang YS, Tsai Y, Jean JS, Li Z, Krukowski K (2013) Removal of ciprofloxacin from water by birnessite. J Hazard Mater 250:362–369. doi:10.1016/j.jhazmat.2013.02.015

4. Ahn Y, Linder SW, Veach BT, Steve Yan S, Haydee Fernandez A, Pineiro SA, Cerniglia CE (2012) In vitro enrofloxacin binding in human fecal slurries. Regul Toxicol Pharmacol: RTP 62(1):74–84. doi:10.1016/j.yrtph.2011.11.013

5. Fengxian C, Reti H (2017) Analysis of positions and substituents on genotoxicity of fluoroquinolones with quantitative structure-activity relationship and 3D Pharmacophore model. Ecotoxicol Environ Saf 136:111–118. doi:10.1016/j.ecoenv.2016.10.036

6. Liu X, Liu Y, Xu J-R, Ren K-J, Meng X-Z (2016) Tracking aquaculture-derived fluoroquinolones in a mangrove wetland, South China. Environ Pollut 219:916–923. doi:10.1016/j.envpol.2016.09.011

7. Golet EM, Alder AC, Hartmann A, Ternes TA, Giger W (2001) Trace determination of fluoroquinolone antibacterial agents in urban wastewater by solid-phase extraction and liquid chromatography with fluorescence detection. Anal Chem 73(15):3632–3638. doi:10.1021/ac0015265

8. Poliwoda A, Krzyzak M, Wieczorek PP (2010) Supported liquid membrane extraction with single hollow fiber for the analysis of fluoroquinolones from environmental surface water samples. J Chromatogr A 1217(22):3590–3597. doi:10.1016/j.chroma.2010.03.051

9. Sun X, He J, Cai G, Lin A, Zheng W, Liu X, Chen L, He X, Zhang Y (2010) Room temperature ionic liquid-mediated molecularly

imprinted polymer monolith for the selective recognition of quino-lones in pork samples. J Sep Sci 33:3786–3793. doi:10.1002/jssc.201000337

10. Marazuela MD, Bogialli S (2009) A review of novel strategies of sample preparation for the determination of antibacterial residues in foodstuffs using liquid chromatography-based analytical methods. Anal Chim Acta 645(1–2):5–17. doi:10.1016/j.aca.2009.04.031

11. Nasiri J, Naghavi MR, Motamedi E, Alizadeh H, Moghadam MRF, Nabizadeh M, Mashouf A (2017) Carbonaceous sorbents alongside an optimized magnetic solid phase extraction (MSPE) towards en-richment of crude Paclitaxel extracts from callus cultures of Taxus baccata. J Chromatogr B 1043:96–106. doi:10.1016/j.jchromb.2016.10.029

12. Fan S, Zhu J, Ren L, Wang M, Bi W, Li H, Huang X, Chen DD (2017) Co-solvent enhanced adsorption with magnetic velvet-like carbon nitride for high efficiency solid phase extraction. Anal Chim Acta 960:63–71. doi:10.1016/j.aca.2017.01.020

13. Hekmatara H, Seifi M, Forooraghi K (2013) Microwave absorption property of aligned MWCNT/Fe_3O_4. J Magn Magn Mater 346:186–191. doi:10.1016/j.jmmm.2013.06.032

14. Ma J, Jiang L, Wu G, Xia Y, Lu W, Li J, Chen L (2016) Determination of six sulfonylurea herbicides in environmental wa-ter samples by magnetic solid-phase extraction using multi-walled carbon nanotubes as adsorbents coupled with high-performance liquid chromatography. J Chromatogr A 1466:12–20. doi:10.1016/j.chroma

15. Cao J, Zhang X, He X, Chen L, Zhang Y (2013) Facile synthesis of a Ni(II)-immobilized core–shell magnetic nanocomposite as an ef-ficient affinity adsorbent for the depletion of abundant proteins from bovine blood. J Mater Chem B 1:3619–3718. doi:10.1039/c3tb20573h

16. Zhang Y, Zhang M, Yang J, Ding L, Zheng J, Xu J, Xiong S (2016) Formation of Fe_3O_4@SiO_2@C/Ni hybrids with enhanced catalytic activity and histidine-rich protein separation. Nanoscale 8:15978–15988. doi:10.1039/C6NR05078F

17. Tang B, Song W-C, Yang E-C, Zhao X-J (2017) MOF-derived Ni-based nanocomposites as robust catalysts for chemoselective hy-drogenation of functionalized nitro compounds. RSC Adv 7(3):1531–1539. doi:10.1039/c6ra26699a

18. Xu X, Nosheen F, Wang X (2016) Ni-decorated molybdenum car-bide hollow structure derived from carbon-coated metal–organic framework for electrocatalytic hydrogen evolution reaction. Chem Mater 28(17):6313–6320. doi:10.1021/acs.chemmater.6b02586

19. Ma J, Yao Z, Hou L, Lu W, Yang Q, Li J, Chen L (2016) Metal organic frameworks (MOFs) for magnetic solid-phase extraction of pyrazole/pyrrole pesticides in environmental water samples follow-ed by HPLC-DAD determination. Talanta 161:686–692. doi:10.1016/j.talanta.2016.09.035

20. Zhou Q, Lei M, Li J, Liu Y, Zhao K, Zhao D (2017) Magnetic solid phase extraction of N- and S-containing polycyclic aro-matic hydrocarbons at ppb levels by using a zerovalent ironnanoscale material modified with a metal organic frame-work of type Fe@MOF-5, and their determination by HPLC. Microchim Acta 184:1029–1036. doi:10.1007/s00604-017-2094-6

21. Chen X, Ding N, Zang H, Yeung H, Zhao R-S, Cheng C, Liu J, Chan TWD (2013) Fe_3O_4@MOF core–shell magnetic micro-spheres for magnetic solid-phase extraction of polychlorinated biphenyls from environmental water samples. J Chromatogr A 1304:241–245. doi:10.1016/j.chroma.2013.06.053

22. Wu Q, Cheng S, Wang C, Li X, Li Z, Hao C (2016) Magnetic porous carbon derived from a zinc-cobaltmetal-organic framework: a adsorbent for magnetic solid phase extraction of flunitrazepam. Microchim Acta 183:3009–3017. doi:10.1007/s00604-016-1948-7

23. Zou F, Chen YM, Liu K, Yu Z, Liang W, Bhaway SM, Gao M, Zhu Y (2016) Metal organic frameworks derived hierarchical hollow NiO/Ni/graphene composites for lithium and sodium storage. ACS Nano 10(1):377–386. doi:10.1021/acsnano.5b05041

24. Carrasco JA, Romero J, Abellan G, Hernandez-Saz J, Molina SI, Marti-Gastaldo C, Coronado E (2016) Small-pore driven high ca-pacitance in a hierarchical carbon via carbonization of Ni-MOF-74 at low temperatures. Chem Commun 52(58):9141–9144. doi:10.1039/c6cc02252a

25. Mukoyoshi M, Kobayashi H, Kusada K, Hayashi M, Yamada T, Maesato M, Taylor JM, Kubota Y, Kato K, Takata M, Yamamoto T, Matsumura S, Kitagawa H (2015) Hybrid materials of Ni NP@MOF prepared by a simple synthetic method. Chem Commun 51(62):12463–12466. doi:10.1039/c5cc04663g

26. Lee G, Lee C, Yoon CM, Kim M, Jang J (2017) High-performance three-dimensional mesoporous graphene electrode for supercapacitors using lyophilization and plasma reduction. ACS Appl Mater Interfaces 9(6):5222–5230. doi:10.1021/acsami.6b13050

27. Wagil M, Kumirska J, Stolte S, Puckowski A, Maszkowska J, Stepnowski P, Bialk-Bielinska A (2014) Development of sensitive and reliable LC-MS/MS methods for the determination of three fluoroquinolones in water and fish tissue samples and preliminary environmental risk assessment of their presence in two rivers in northern Poland. Sci Total Environ 493:1006–1013. doi:10.1016/j.scitotenv.2014.06.082

28. Tang Y, Guo H, Xiao L, Yu S, Gao N, Wang Y (2013) Synthesis of reduced graphene oxide/magnetite composites and investigation of their adsorption performance of fluoroquinolone antibiotics. Colloids Surf A Physicochem Eng Asp 424:74–80. doi:10.1016/j.colsurfa.2013.02.030

29. Zhou Q, Zhu L, Xia X, Tang H (2016) The water – resistant zeolite imidazolate framework 67 is a viable solid phase sor-bent for fluoroquinolones while efficiently excluding macro-molecules. Microchim Acta 183(6):1839–1846. doi:10.1007/s00604-016-1814-7

30. Wu X, Huang M, Zhou T, Mao J (2016) Recognizing removal of norfloxacin by novel magnetic molecular imprinted chitosan/γ-Fe_2O_3 composites: Selective adsorption mechanisms, practi-cal application and regeneration. Sep Purif Technol 165:92–100. doi:10.1016/j.seppur.20 16.03.04

31. Andrea S, Michela S, Federica M, Elettra M, Dhanalakshmi V, Daniele D, Antonella P (2016) Preparation of silica-supported car-bon by Kraft lignin pyrolysis, and its use in solid-phase extraction of fluoroquinolone from environmental waters. Microchim Acta 183:2241–2249. doi:10.1007/s00604-016-1859-7

32. Wang R, Yuan Y, Yang X, Han Y, Yan H (2015) Polymethacrylate microparticles covalently functionalized with an ionic liquid for solid-phase extraction of fluoroquin-olone antibiotics. Microchim Acta 182:2201–2208. doi:10.1007/s00604-015-1544-2

33. Parirokh L, Noor M, Mohammad R, Khalil A, Seyed M (2017) Colorimetric aptamer based assay for the determination of fluoroquinolones by triggering the reduction-catalyzing activi-ty of gold nanoparticles. Microchim Acta 184:2039–2045. doi:10.1007/s00604-017-2213-4